

# INTERNATIONAL SOCIETY FOR SOIL MECHANICS AND GEOTECHNICAL ENGINEERING



*This paper was downloaded from the Online Library of the International Society for Soil Mechanics and Geotechnical Engineering (ISSMGE). The library is available here:*

<https://www.issmge.org/publications/online-library>

*This is an open-access database that archives thousands of papers published under the Auspices of the ISSMGE and maintained by the Innovation and Development Committee of ISSMGE.*

## NON-LINEAR COUPLED APPROACH FOR THE EVALUATION OF SEISMIC SLOPE DISPLACEMENTS

Giuseppe TROPEANO<sup>1</sup>, Ernesto AUSILIO<sup>2</sup>, Antonio COSTANZO<sup>3</sup>

### ABSTRACT

The design procedures to evaluate earthquake-induced sliding displacements typically refer to three different approaches: simplified methods; displacements methods and advanced dynamic methods. In the first class of methods, empirical relationships are used to predict the permanent slope displacement. The second class includes simplified dynamic analysis, by means of the conventional Newmark rigid block model, as well as through its improvements to account for soil deformability. The dynamic site response and the sliding block displacements are computed separately in the “decoupled” approach or simultaneously in the “coupled” analysis (stick-slip model). The advanced dynamic methods are based on finite element (FEM) or finite difference (FDM) formulations, which permit to account for topography and heterogeneity by two or three dimensional analysis.

The paper describes the developments of a 1D lumped-mass stick-slip model for a layered subsoil including more generalized assumptions than a previous version (Ausilio et al., 2008). The depth of the sliding surface is considered not necessarily coincident with that of the bedrock, and located in a generic layer. This latter can be identified during the analysis.

In the non-linear site response analysis, a recent soil damping formulation was used (Phillips & Hashash, 2009). In this formulation, a reduction factor modifying the extended Masing loading/unloading strain-stress relationship was introduced. The predictions of the coupled stick-slip model with non-linear soil behaviour were compared with the results of the equivalent linear approach for ideal slopes to show the effects of non linearity on seismic performance. Besides, the results show that the sliding surface depth, automatically researched, is function of main ground motion parameters.

Keywords: seismic slope stability, displacements, numerical analysis, coupled approach

### INTRODUCTION

The seismic performance of slopes is assessed by calculating the permanent earthquake induced displacements. The usual procedures to estimate the seismic displacements refer to three different approaches of increasing complexity: 1) simplified methods based on empirical-statistical relationships (e.g. Bray et al., 1998, Tropeano et al., 2009), 2) displacement based analysis in which the permanent displacements induced by earthquake acceleration time history are predicted, 3) advanced dynamic methods based on finite element (FEM) or finite difference (FDM) formulations, which permit to account for topography and heterogeneity by two or three-dimensional analyses.

The displacement based analysis includes simplified dynamic analysis by means of the conventional Newmark rigid block model (Newmark, 1965) as well as through its improvements to account for soil deformability with decoupled and coupled models.

---

<sup>1</sup> Ph.D., DDS, University of Calabria, Italy, e-mail: tropeano@dds.unical.it

<sup>2</sup> Assistant Professor, DDS, University of Calabria, Italy, e-mail: ausilio@dds.unical.it

<sup>3</sup> Ph.D., DDS, University of Calabria, Italy, e-mail: acostanzo@dds.unical.it

The decoupled model assumes that dynamic response and sliding response analyses can be performed separately. In the coupled approach the wave propagation and sliding block analyses are performed simultaneously. The coupled approach was numerically modelled using different formulations to describe the behaviour of soil.

Lin and Whitman (1983) used a lumped-mass shear beam model with linear elastic soil properties.

Chopra and Zhang (1991) applied the method to the analysis of a concrete gravity dam. They used a generalized single degree of freedom (SDOF) procedure, with mass and elasticity distributed along the height of a dam. Gazetas and Uddin (1994) implemented the coupled sliding into a 2D linear-equivalent finite element program. Kramer and Smith (1997) used a non linear discrete mass model with two masses, connected by a spring and a dashpot, with the lower mass that can slide along an underlying inclined plane. Rathje and Bray (1999) proposed a layered “stick-slip” model to compute coupled sliding displacements of geotechnical structures, with linear or equivalent-linear material properties. The same authors updated the model to a multi-degree-of-freedom (MDOF) system, accounting for the fully non-linear material response (Rathje and Bray, 2000).

Ausilio et al. (2008) implemented a lumped-mass stick-slip model with more generalized assumptions in which the depth of the sliding surface,  $H_s$ , may be located in a generic layer (Figure 1). Moreover, the bedrock can be considered deformable. This model was implemented in a first version of a computation code that used a linear equivalent formulation.

This paper describes the developments of the previous version of computation code proposed by Ausilio et al. (2008). In the non-linear site response analysis, a recent soil damping formulation was used (Phillips and Hashah, 2009). In this formulation, a reduction factor modifying the extended Masing loading/unloading strain-stress relationship was introduced. To verify the non-linear behaviour effects introduced by the above-mentioned formulation both into dynamic analyses and cumulated displacements, the results are compared with those obtained using different approaches.

Besides, as regards the depth of sliding surface it is not imposed but it may be sought automatically.

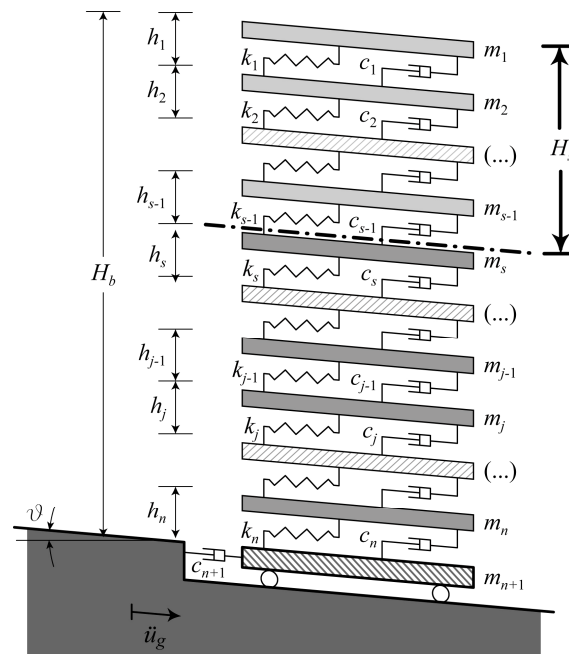


Figure 1. The MDOF system used in this study.

COUPLED APPROACH

The stick slip model

The analytic stick-slip model is based on two dynamic phases: in the first one the unstable mass cumulates potential energy that is transformed in movement during the second phase.

In the stick phase, the seismic response of the lumped mass scheme used in this study (Figure 1) in terms of absolute displacements,  $\mathbf{u}_a$ , to a base ground motion,  $\ddot{u}_g$ , can be computed by integrating the following system:

$$\mathbf{M} \cdot \ddot{\mathbf{u}}_a + \mathbf{C} \cdot \dot{\mathbf{u}}_a + \mathbf{K} \cdot \mathbf{u}_a = \mathbf{i} \cdot c_{n+1} \cdot \dot{u}_g \quad (1)$$

where  $\mathbf{M}$ ,  $\mathbf{C}$  and  $\mathbf{K}$  are the mass, damping and stiffness matrices, and  $c_{n+1} = \rho_r V_{s,r}$  is the seismic impedance of the bedrock;  $\mathbf{i}$  is a vector with each element equal to zero, except for the  $(n+1)$ -th that is equal to unity.

The shear critical strength at the sliding surface can be expressed as  $m_T a_y$ , where  $m_T$  is the total mass above the sliding surface, and  $a_y$  is the yield acceleration of the slope. The forces acting on the sliding interface (Figure 2) are:

$$-m_T \cdot \ddot{u}_s - \mathbf{1}^T \mathbf{M}_S \cdot \ddot{\mathbf{u}} \quad (2)$$

The first term is the inertial force induced by the absolute acceleration at  $s$ -th layer,  $\ddot{u}_s$ , while the second is that resulting from the non-uniform relative acceleration profile,  $\ddot{\mathbf{u}}$ , within the sliding mass, referred to  $\ddot{u}_s$ . The subscript "S" indicates sub-matrices and sub-vectors with index from 1 to  $(s-1)$  for the sliding part of the dynamic system.  $\mathbf{1}$  is the unity vector.

The "slip" conditions start when the inertia forces are equal the resisting force corresponding to the product of the sliding mass and the yield acceleration  $m_T a_y$ . In such a case the equation of motion for the deformable mass above the sliding surface is given by the expression:

$$\mathbf{M}_S \ddot{\mathbf{u}} + \mathbf{C}_S \dot{\mathbf{u}} + \mathbf{K}_S \mathbf{u} = -\mathbf{M}_S \cdot \mathbf{1} \cdot (\ddot{u}_s + \ddot{u}_0) \quad (3)$$

On the sliding surface the equilibrium, during the slip, is governed by the condition:

$$-m_T \cdot (\ddot{u}_s + \ddot{u}_0) - \mathbf{1}^T \mathbf{M}_S \cdot \ddot{\mathbf{u}} = m_T \cdot a_y \quad (4)$$

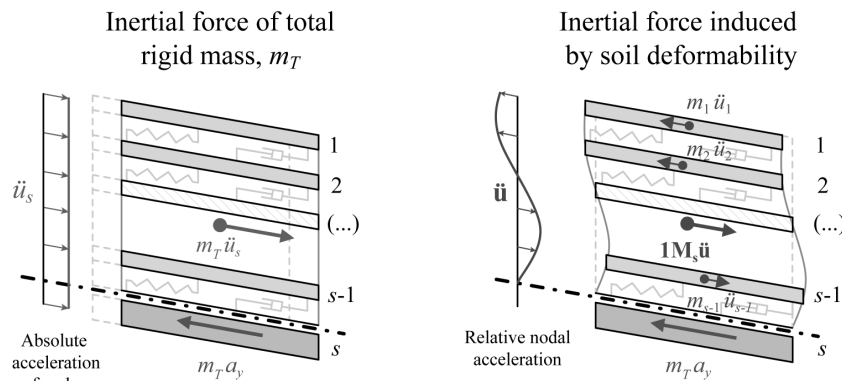


Figure 2. Forces acting on sliding deformable mass.

Substituting eq. (4) in eq. (3), the equation for the “slip” conditions is obtained as:

$$\mathbf{M}^* \ddot{\mathbf{u}} + \mathbf{C}_s \dot{\mathbf{u}} + \mathbf{K}_s \mathbf{u} = \mathbf{M}_s \cdot \mathbf{1} \cdot a_y \quad (5)$$

where  $\mathbf{M}^*$  is defined as:

$$\mathbf{M}^* = \mathbf{M}_s - \frac{1}{m_T} \mathbf{M}_s \cdot \mathbf{1} \cdot \mathbf{1}^T \mathbf{M}_s \quad (6)$$

Solving eq. (5) in terms of nodal relative acceleration,  $\ddot{\mathbf{u}}$ , the sliding acceleration time histories are obtained from eq. (4) as:

$$\ddot{u}_0 = -a_y - \frac{1}{m_T} \cdot \mathbf{1}^T \mathbf{M}_s \cdot \ddot{\mathbf{u}} - \ddot{u}_s \quad (7)$$

The sliding displacement,  $u_0$ , is computed by integrating twice eq. (7) until sliding velocity,  $\dot{u}_0$ , becomes equal to zero.

The position of critical sliding surface,  $H_s$ , for the computation of permanent displacements, may be identified in the layer where is tested out for the first time the condition represented in the eq. (4).

### Numerical implementation

The above model was implemented in a numerical code (ACST). The code optimizes the input data procedure and the outputs resulting from the analyses.

The discretization of subsoil profile is done automatically on the basis of Lysmer and Kuhlemeyer (1969) criteria as function of shear wave velocity and maximum frequency of input motion.

Setting the number of sublayer of numerical model, the elements of the matrices  $\mathbf{M}$  and  $\mathbf{K}$  are defined from the mass,  $m_j$ , and the spring stiffness,  $k_j$ , for a generic layer  $j$ , as follows:

$$m_1 = \frac{\rho_1 h_1}{2}; \quad m_j = \frac{\rho_j h_j + \rho_{j-1} h_{j-1}}{2}; \quad m_{n+1} = \frac{\rho_n h_n}{2} \quad (8)$$

$$k_j = \frac{G_j}{h_j} \quad (9)$$

where  $\rho_j$ ,  $h_j$ , and  $G_j$  are the density, thickness and shear stiffness of the  $j$ -th layer.

The viscous damping matrix,  $\mathbf{C}$ , is defined according to the full Rayleigh damping formulation (Hashash and Park, 2002):

$$\mathbf{C} = \alpha_R \mathbf{M} + \beta_R \mathbf{K} \quad (10)$$

The constants  $\alpha_R$  and  $\beta_R$  are functions of the soil damping ratio,  $\zeta$ , the first natural frequency of the subsoil profile and the predominant frequency of input motion.

In the computer code implemented in this work, the non-linear hysteretic response of the soil was modelled with extended modified Kondor-Zelasko (MKZ) hyperbolic model. MKZ is defined by two equations for loading and for unloading-reloading conditions. Eq. (11) defines the stress-strain relationship (backbone curve) for loading:

$$F_{bb}(\gamma) = \frac{\gamma G_0}{1 + \beta(\gamma/\gamma_r)^s} \quad (11)$$

where,  $\gamma$  is the given shear strain,  $G_0$  is the initial shear modulus,  $\gamma_r$  is the reference shear strain and  $\beta$  and  $s$  are two dimensionless factors.

For the stress-strain relationship for unloading-reloading condition, it was referred to a recent formulation proposed by Phillips and Hashash (2009):

$$\tau = F(\gamma_m) \cdot \left[ \frac{G_0(\gamma - \gamma_c)}{1 + \beta \left( \frac{\gamma - \gamma_c}{2\gamma_r} \right)^s} - \frac{G_0(\gamma - \gamma_c)}{1 + \beta \left( \frac{\gamma_m}{2\gamma_r} \right)^s} \right] + \frac{G_0(\gamma - \gamma_c)}{1 + \beta \left( \frac{\gamma_m}{2\gamma_r} \right)^s} + \tau_c \quad (12)$$

where,  $\gamma_c$  and  $\tau_c$  are respectively the reversal shear strain and shear stress,  $\gamma_m$  is the maximum shear strain and  $F(\gamma_m)$  is a damping reduction factor defined as follows:

$$F(\gamma_m) = \frac{\xi_{measured}}{\xi_{Masing}} = p_1 - p_2 \left( 1 - \frac{G(\gamma_m)}{G_0} \right)^{p_3} \quad (13)$$

in which  $p_1$ ,  $p_2$  and  $p_3$  are non-dimensional parameters obtained from the best fit of the ratio between the hysteretic damping measured in laboratory tests,  $\xi_{measured}$ , and those calculated using the Masing rules,  $\xi_{Masing}$ .  $G(\gamma_m)$  is the secant modulus corresponding to the maximum shear strain level  $\gamma_m$ .

This new expression modifies the Masing unloading-reloading rules and it provides a better agreement with the damping curves for larger shear strains. In the numerical implementation, the application of the factor  $F(\gamma_m)$  introduces, also, a sensitive reduction of shear stiffness, that could be assumed as a parameter of degradation.

ACST uses the Newmark  $\beta$  method (Newmark, 1959) to solve numerically at each time step the equation of motion for both the analysis phases. In this paper, the coefficients of  $\beta$ -method which govern the stability, accuracy and numerical dissipation of the integration method, are chosen in order that the method is unconditionally stable and there no numerical damping.

In the code ACST are implemented different options about the position of sliding surface that can be imposed before the starting of analyses or it can be sought automatically.

## APPLICATIONS AND RESULTS

The above method was applied to the infinite slope models used by Ausilio et al. (2008), constituted by two medium-plasticity clay subsoils: the first normally consolidated (NC) and second heavily over-consolidated (OC). The basic soil parameters are summarized in the table shown in Figure 3c. The constitutive parameters were assumed with values typical for a clay soil with  $IP = 30\%$ .

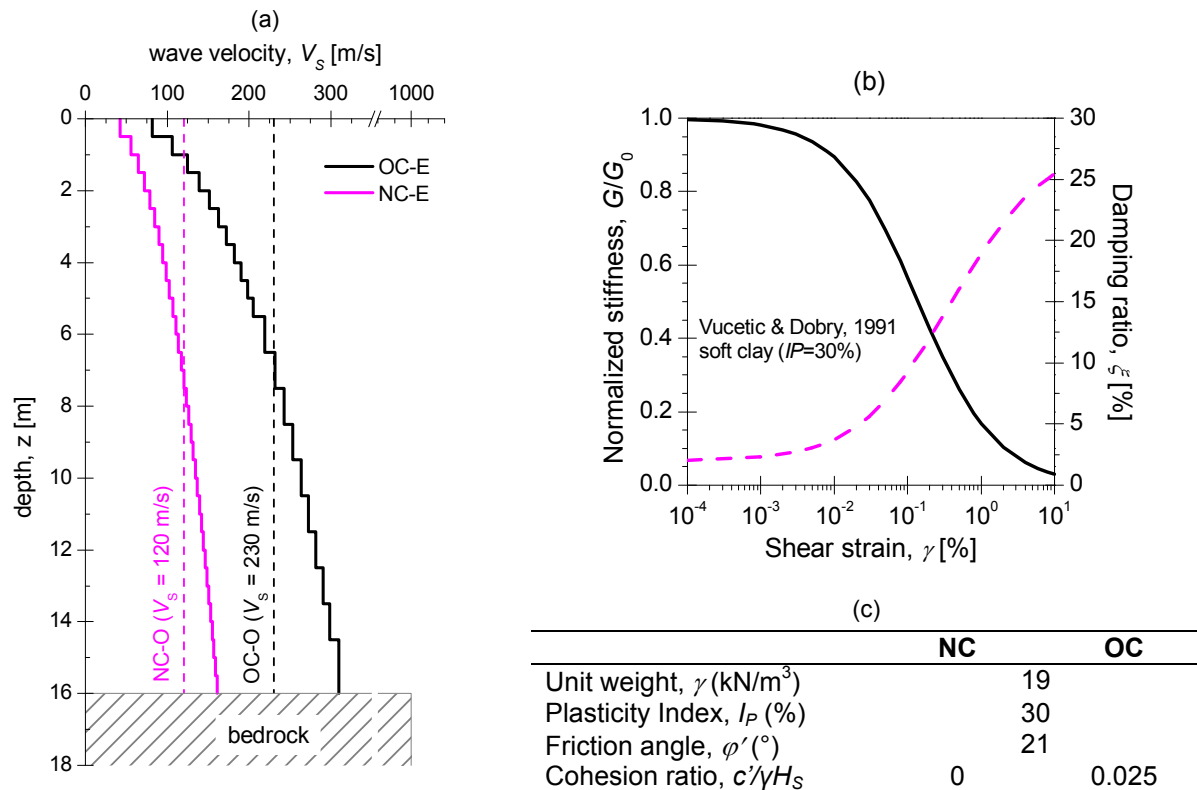


**Figure 3. Shear wave velocity profile (a), variation of normalised stiffness and damping with shear strain (b) and main geotechnical parameters (c) assumed for the clay subsoils.**

The same friction angle,  $\phi'$ , and different effective cohesion ratio,  $c'/\gamma H_s$ , were assumed for the NC and OC clay subsoils. Thus, the yield acceleration values,  $a_y$ , computed for an infinite slope model, resulted constant with depth and equal to 0.017g and 0.042g, respectively for NC and OC subsoil.

Two different profiles of shear wave velocity,  $V_s$ , was considered for both subsoils: 1) constant value of  $V_s$  with the depth: homogeneous soil (O) (Figure 3a); 2) heterogeneous variation of  $V_s$  with depth using the relationships proposed by Rampello et al. (1994) (E - Figure 3a).

The discretization of the soil profiles was optimized in order to get the best reproduction of earthquake frequencies as high as 25 Hz. The strain-dependent shear modulus and damping curves, representing the non-linear soil behaviour, were based on those suggested by Vucetic and Dobry (1991) for clays with  $IP = 30\%$  (Figure 3b).

In all the analyses, the bedrock was assumed at a constant depth ( $H_b = 16$  m), with a unit weight of 22 kN/m<sup>3</sup> and a shear wave velocity equal to 1000 m/s. The bedrock input motion was the NS component of the Borgo Cerreto-Torre record (peak acceleration,  $a_{max} = 0.185g$ , median period,  $T_m = 0.154$  s) of the 1997 Umbria-Marche earthquake ( $M_w = 5.7$ ).

In Figure 4, the results of the seismic site response (SSR), in no-slip conditions, predicted using the numerical code implemented in this study in terms of maximum acceleration (Figure 4a), shear strain (Figure 4b) and shear stress (Figure 4c) profiles for NC-E clay subsoil are summarized. The results was compared with those obtained in a previous work (Ausilio et al., 2008) with linear equivalent analysis with the aim to evaluate the effect of non-linear formulation into the SSR.

In the same figure, also, the results of SSR analyses obtained with a common non-linear code (NERA, Bardet and Tobita, 2001) are shown. The same comparison is shown in Figure 5 for OC-E clay subsoil.

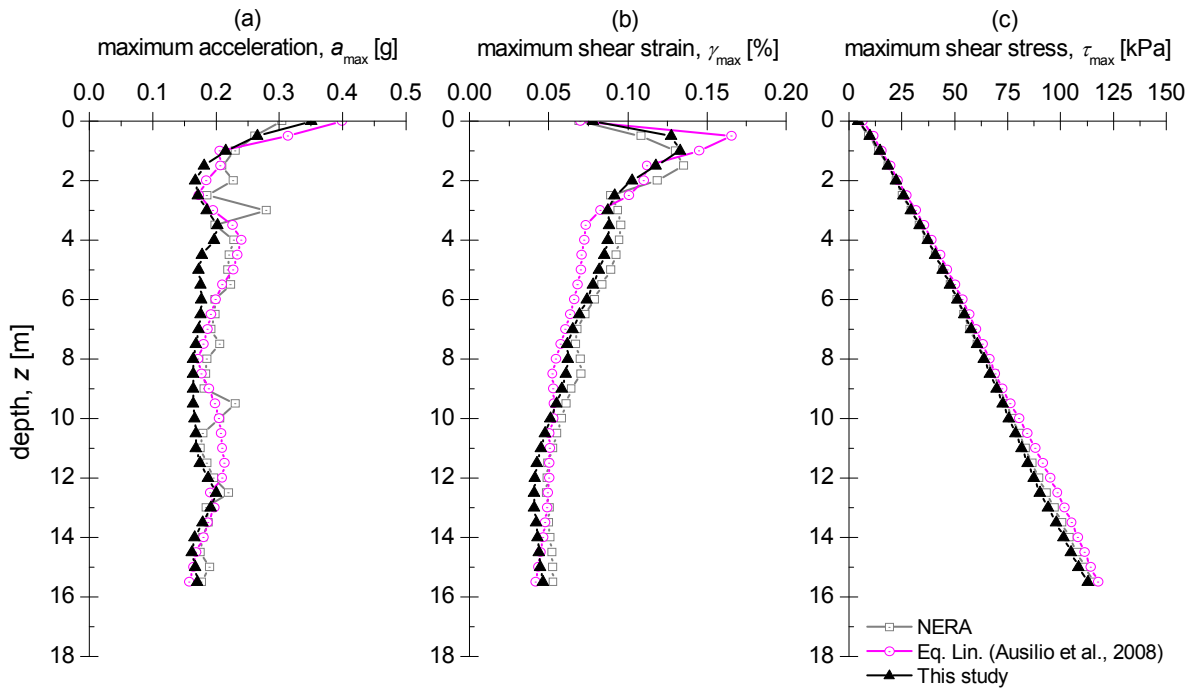


**Figure 4. 1D seismic site response computed by NERA, equivalent linear soil behaviour formulation (Ausilio et al., 2008) and non linear incremental formulation (this study) for NC-E clay soil: profiles of peak acceleration (a) shear strain (b) and shear stress (c).**

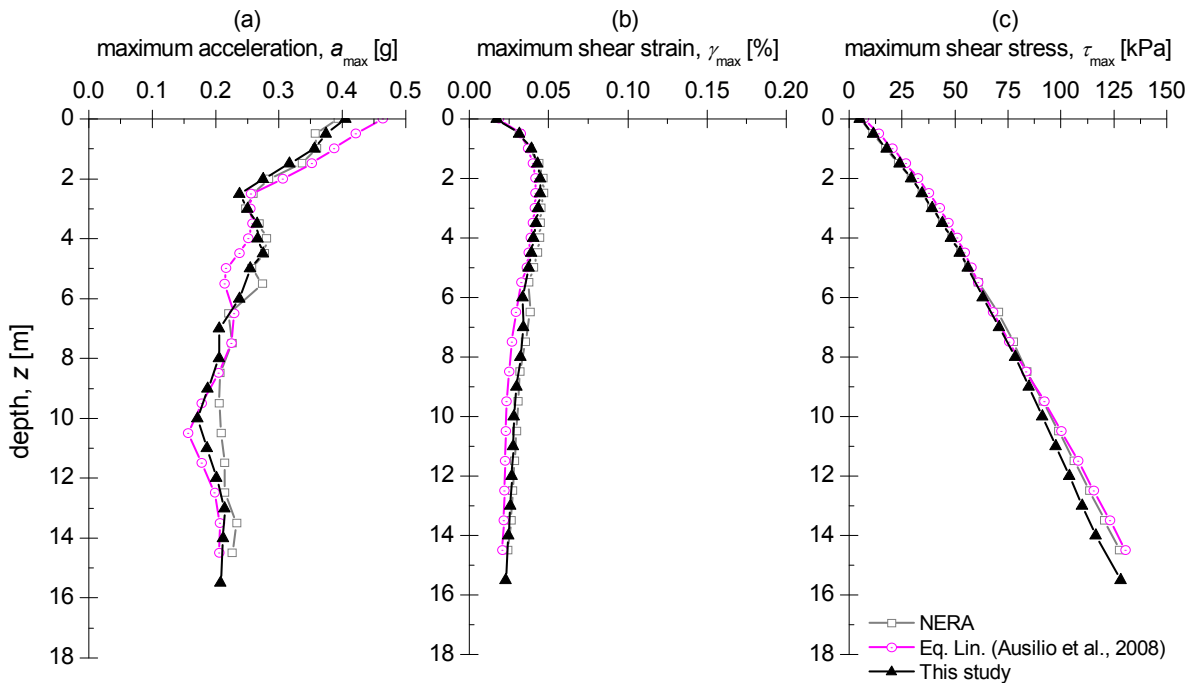


**Figure 5. 1D seismic site response computed by NERA, equivalent linear soil behaviour formulation (Ausilio et al., 2008) and non linear incremental formulation (this study) for OC-E clay soil: profiles of peak acceleration (a) shear strain (b) and shear stress (c).**



The linear equivalent analyses overestimate the maximum acceleration in the uppermost layers for both subsoil type. The maximum shear strain profiles obtained using the two approaches are similar for the stiffer OC clay while for the NC soil the trend is quite different. This could be due to the more pronounced non-linear effects in the NC soil, being the shear strain even higher than 0.1%, instead the OC clay shows a stiffer and more linear behaviour ( $\gamma < 0.05\%$ ).

As regards the shear stress profiles the differences are less pronounced. Generally the response of soil using non-linear analyses in the uppermost layers is lower than those obtained with the equivalent linear approach.

For the computation of displacements, the depth of the sliding surfaces,  $H_s$ , is imposed equal to 5, 10 and 15m for both subsoil models.

The permanent sliding displacements obtained in this study, using non-linear soil properties in to the coupled approach, are compared, in Figure 6, with those resulting from an equivalent linear coupled approach (Ausilio et al., 2008) for shallow (a, d), intermediate (b, e) and deep (c, f) sliding surfaces.

The Figure 6 reveals that the displacements from non linear coupled analysis are smaller than those obtained from equivalent linear analysis. However, this difference becomes more significant for the softer NC soil and it decreases when the ratio between the natural period of the unstable soil,  $T_s$ , and the median period of input motion,  $T_m$ , increases (Figure 6a, b, c). The same trend is observed also for stiffer OC clay but with moderate degree.

The use of equivalent linear model in a coupled sliding analyses could bring to a significant over prediction of permanent displacements above all for softer and more deformable soil and for smaller depths of sliding surfaces.

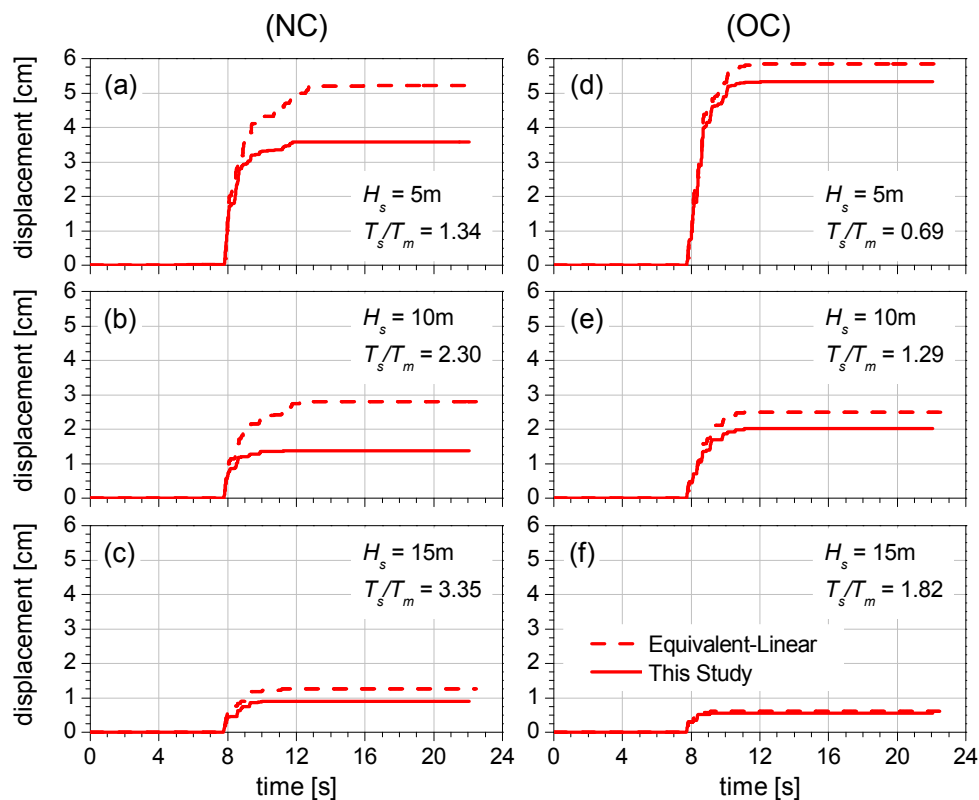
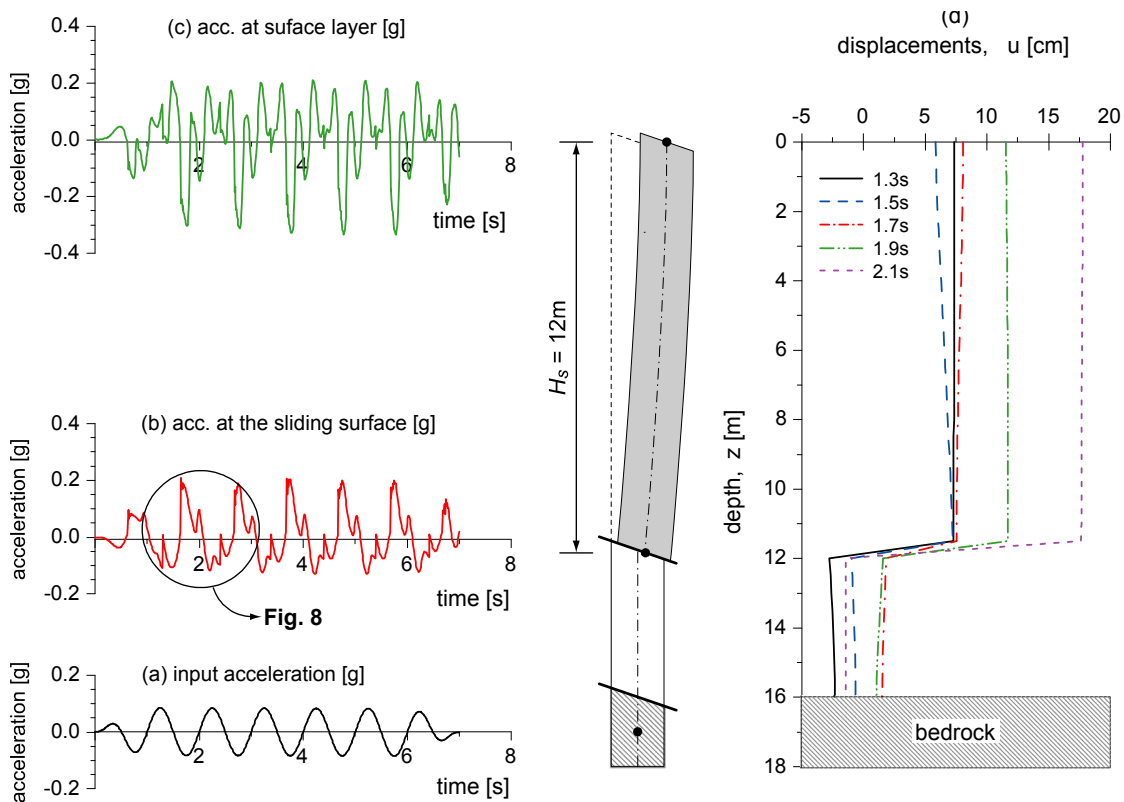


Figure 6. Comparison between cumulated displacement computed with linear equivalent analyses and with non linear analyses at variable depth of sliding surface.

**Slip surface**

To highlight the different possible locations of critical sliding surface, some analyses was performed considering the subsoils described in the previous section.

Regarding the bedrock input motion was used a sine wave with amplitude function of yield acceleration,  $a_y$ , frequency between 0.5 and 5 Hz, and a constant number of cycles, with the first and last one modulated in amplitude with two sigmoid laws.



**Figure 7. Example of NC clay subsoil subjected to a synthetic accelerogram (a) with frequency 1Hz: acceleration time histories obtained at sliding surface depth (b), at surface layer (c) and the instantaneous displacements profiles (d).**

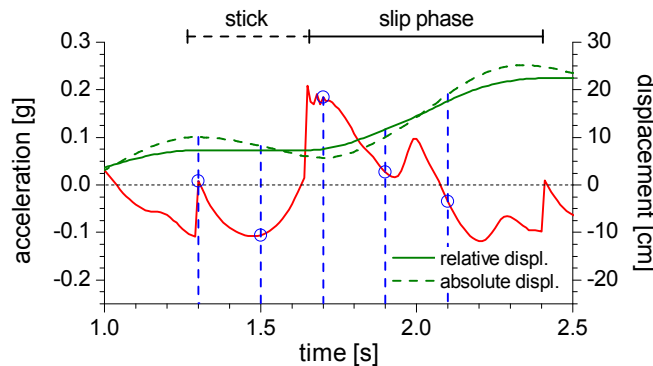


**Figure 8. Detail of acceleration time history at sliding surface layer around the time instant considered in Figure 7d.**

In Figure 7, the acceleration time history input at bedrock layer (Figure 7a) and those obtained at first sliding surface depth (Figure 7b) and at layer surface (Figure 7c) are shown. In the same figure, the profiles of displacements for different instants are, also, displayed. These profiles highlight that the depth of sliding surface is located at 12m depth. The Figure 8 shows a detail of acceleration time history and cumulated displacements at sliding surface layer to explain what occurs during the stick and slip phases.

At the time  $t = 1.3\text{s}$  the unstable mass, that has cumulated about 5cm from the previous slip phase, is in stick condition until a new triggering of motion occurs at the time 1.7s (Figure 8). During this lapse the soil can response to dynamic input with upstream instantaneous displacements. Starting by  $t = 1.7\text{s}$ , a new slip stage with graduate increase of displacement along sliding surface, occurs. The scale of displacements in Figure 7d doesn't allow to show the deformation of soil column. This latter, anyway, plays an important role in the computation of acceleration time history at sliding surface depth (Figure 8).

In Figure 9a the stress-strain cycles for the forementioned analysis of the soil layer directly upon the sliding surface are shown. Starting from lithostatic stress,  $\tau_0$ , the soil responses to the dynamic action with a stress-strain pattern in accord with the Masing rules, until the rupture limits stress,  $\tau_{cr}$ , is reached. This value is held constant during the sliding. During slip phase, the soil accumulates small strain to which higher value of stiffness are associated according to Masing rules.

The time history of shear stiffness,  $G$ , of the soil layer upon the sliding surface normalized with initial maximum stiffness,  $G_0$ , is reported in Figure 9b. In this case, it would be highlighted the reduction of about 13% of normalized shear modulus induced by the Phillips and Hashash (2009) formulation until the shear strain of soil layer doesn't reach the maximum value.

The Figure 10 shows the relationship between the first sliding surface depth,  $H_s$ , normalized with the bedrock depth,  $H_b$ , and the ratio of the fundamental period of unstable soil,  $T_s$ , and the input motion period,  $T$ .

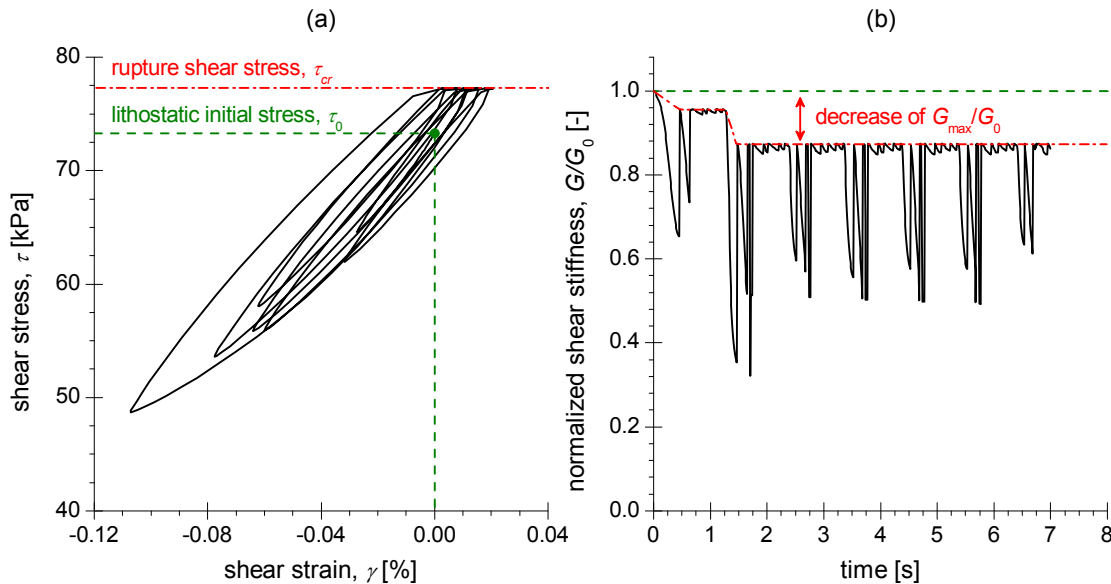


**Figure 9. Example of hysteretic cycle (a) and time history of shear stiffness (b) at the layer of sliding surface for NC clay subjected to a synthetic accelerogram with frequency 1Hz.**

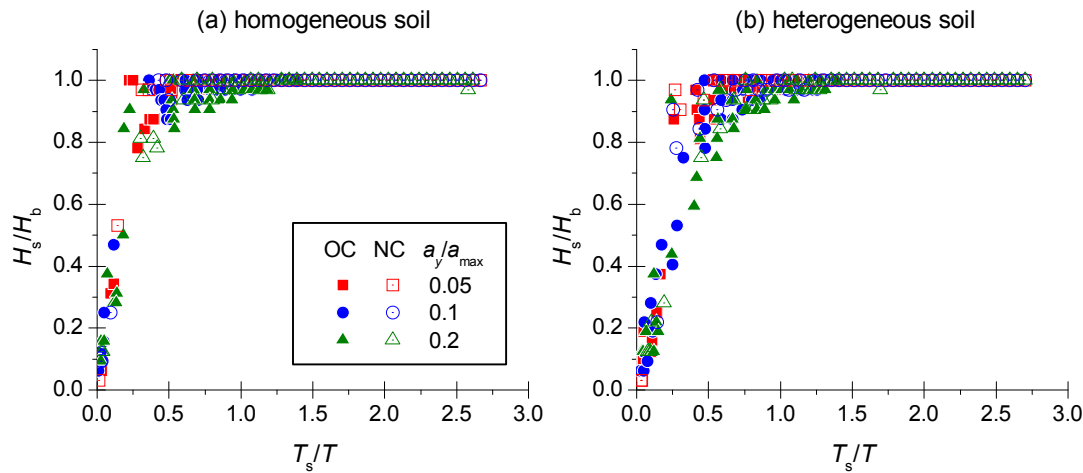


**Figure 10. Normalized sliding surface depth,  $H_s/H_b$ , versus period ratio varying subsoil type and peak ground acceleration for homogeneous (a) and heterogeneous (b) soil.**

The value of  $H_s$  was computed for all the subsoil described in Figure 3 and for acceleration ratio (i.e. the ratio of yield acceleration,  $a_y$ , and maximum of input motion,  $a_{max}$ ) value equal to 0.05, 0.1 and 0.2. The normalized sliding surface depth tends to increase with the period ratio until  $H_s$  doesn't reach the bedrock depth. This condition is verified for a specified value of  $T_s/T$  that increases with the increasing of acceleration ratio; on the other hand it tends to decrease for more deformable soil.

This trend is observed for both the homogeneous soil profiles Figure 10a and the heterogeneous ones Figure 10b.

## CONCLUSIONS

A non-linear lumped mass coupled model was presented for the 1D dynamic site response analyses and the computation of cumulated displacements. This application could be addressed to evaluate the seismic performance of different geotechnical structures in which the problem could be assimilated as 1D analyses (i.e. infinite slope, landfill). The lumped mass formulation allows, also, the possibility to include simplified structural elements. The recent proposal of Phillips and Hashash (2009) that considers a reduction factor modifying the extended Masing loading/unloading strain-stress relationships, was introduced to model the non linear hysteretic behaviour of soil. Besides, a procedure was implemented for automatically detecting the sliding surface as the first layer in which rupture limited state occurs for the first time.

The comparison with equivalent linear analyses indicates that non linear effects are significant above all in the uppermost layers where the motion amplitudes could be significantly decreased by the higher deformations. The non linearity, also, effects the sliding displacements. The non linear coupled sliding displacements were compared with displacements computed with linear equivalent analyses, showing that the linear equivalent model could be significantly conservative especially for the softer soils and for shallow sliding surfaces.

Finally the first results of the analyses of simplified model show that the position of sliding surface depend, also, on the seismic input. In particular the period,  $T$ , in relation to fundamental period of soil column,  $T_s$ , seems to play the main role. In fact, for low values of the ratio  $T_s/T$ , associated to a stiffer

response of unstable soil, the sliding occurs in superficial layer while for high values of this ratio the sliding starts at the interface of soil-bedrock.

## REFERENCES

- Ausilio, E., Costanzo, A., Silvestri, F., Tropeano, G. (2008). "Prediction of seismic slope displacements by dynamic stick-slip analyses". Proc. MERCEA'08, Reggio Calabria and Messina, Italy, July 8-11, 2008.
- Bardet, J. P., Tobita, T. (2001). "NERA a Computer Program for Nonlinear Earthquake site Response Analyses of Layered Soil Deposits". Univ. of Southern California, Dep. of Civil Eng.
- Bray, J.D., Rathje, E.M., Augello, A.J., Merry, S.M. (1998). "Simplified seismic design procedure for geosynthetic-lined - solid-waste landfills". *Geosynthetics International*, 5 (1-2), 203-235.
- Chopra, A. K., Zhang, L. (1991). "Earthquake-Induced base sliding of concrete gravity dams". *Journal of Structural Engineering*, 117 (12), 3698-3719.
- Gazetas, G., Uddin, N. (1994). "Permanent deformation on preexisting sliding surfaces in dams". *Journal of Geotechnical Engineering, ASCE*, 120 (11), 2041–2061.
- Hashash, Y.M.A., Park, D. (2002). "Viscous damping formulation and high frequency motion propagation in non-linear site response analysis". *Soil Dynamics and Earthquake Engineering*, 22, 611–624.
- Kramer, S. L., Smith, M. W. (1997). "Modified Newmark model for seismic displacements of compliant slopes". *J. Geotech. Geoenviron. Eng.*, 123 (7), 635–644.
- Lin, J.S., Whitman, R.V. (1983). "Decoupling Approximation to the Evaluation of Earthquake-Induced Plastic Slip in Earth Dams". *Earthquake Engineering and Structural Dynamics*, 11, 67-678.
- Lysmer, J., Kuhlemeyer, L., (1969). "Finite dynamic model for infinite media". *Journal of the Engineering Mechanics Division*, 859-877.
- Makdisi, F.I., Seed, H.B. (1978). "Simplified procedure for estimating dam and embankment earthquake-induced deformations". *J. Geotechnical Engrg., ASCE*, 104 (7), 849-867.
- Newmark, N.M. (1959). "A method of computation for structural dynamics". *ASCE J. of the Engineering Mechanics Division*, 85 (EM 3), 67–94.
- Newmark, N.W. (1965). "Effects of earthquakes on dams and embankments". *The V Rankine Lecture of the British Geotechnical Society, Géotechnique*, 15 (2), 139-160.
- Phillips, C., Hashash, Y.M.A. (2009). "Damping formulation for non linear 1D site response analyses". *Soil Dynamics and Earthquake Engineering*, 29, 1143–1158.
- Rampello, S., Silvestri, F., Viggiani, G. (1994). "The dependence of small stress strain stiffness on stress state and history for fine grained soils: the example of Vallericca clay". *Proc. of Intern. Symp. On Pre-failure deformation of geomaterials, IS-Hokkaido*, 1, 273-279, Balkema
- Rathje, E. M., Bray, J. D. (1999). "An examination of simplified earthquake-induced displacement procedures for earth structures". *Canadian Geotechnical Journal*, 36, 72–87.
- Rathje, E. M., Bray, J. D. (2000). "Nonlinear coupled seismic sliding analysis of earth structures". *J. Geotech. Geoenviron. Eng.*, 126 (11), 1002–1014.
- Tropeano, G., Ausilio, E., Costanzo, A., Silvestri, F. (2009). "Valutazione della stabilità sismica di pendii naturali mediante un approccio semplificato agli spostamenti". XIII Convegno Nazionale "L'Ingegneria Sismica in Italia (ANIDIS 2009)", Bologna, 28 Giugno – 2 Luglio 2009.
- Vucetic, M., Dobry, R. (1991). "Effect of soil plasticity on cyclic response". *Journal of Geotechnical Engineering, ASCE*, Vol. 117, No.1, pp. 89-107.